Anticipated Spin Susceptibility Characteristics of the A-10 Aircraft

K.L. Johnson* and Thomas B. Willen†
Aeronautical Systems Division, Wright-Patterson Air Force Base, Ohio

This paper presents the results of a real-time six-degree-of-freedom computer analysis of the spin entry, spin, and recovery characteristics of the U.S. Air Force A-10 close air-support aircraft. The primary emphasis of this study was directed toward determination of the spin susceptibility of the A-10 aircraft during 1-*g* trim and accelerated flight conditions. The computer analysis was based upon 640 wind-tunnel test hours on 1/10- and 1/20-scale models of the prototype A-10 aircraft at high angles of attack. The analysis approach followed guidelines of the U.S. Air Force specification, MIL-S-83691A, "Stall/Post-Stall/Spin Flight Test Demonstration Requirements." The results indicated that three spin modes exist for the A-10 aircraft but that only one of these spin modes (a low angle-of-attack spin mode) could be entered with misapplied control inputs from 1-*g* trim or accelerated flight conditons. The exception to this statement was the fully extended speedbrake configuration, where two spin modes were obtained from a 1-*g* trim flight condition. Recoveries from all spin modes were shown to be excellent except for the high angle-of-attack spin mode, where these results were inconclusive.

Nomenclature

b	= reference wing span
$\bar{c}$	= mean aerodynamic chord
C_l	= aerodynamic roll moment coefficient
C_{l_r}	= roll moment due to yaw rate derivative
C_{l_β}	= roll moment due to sideslip derivative
$C_{l_{\delta_a}}$	= roll moment due to aileron derivative
C_m	= aerodynamic pitch moment coefficient
C_{m_q}	= pitch moment due to pitch rate derivative
C_{m_α}	= pitch moment due to angle-of-attack derivative
$C_{m_{\delta_e}}$	= pitch moment due to elevator derivative
C_N	= body axis normal force coefficient
C_n	= aerodynamic yaw moment coefficient
C_{n_p}	= yaw moment due to roll rate derivative
C_{n_r}	= yaw moment due to yaw rate derivative
C_{n_β}	= yaw moment due to sideslip derivative
$C_{n_{\delta_a}}$	= yaw moment due to aileron derivative
$C_{n_{\delta_r}}$	= yaw moment due to rudder derivative
g	= gravitational constant
I_x, I_y, I_z	= moments of inertia about the x,y, and z body axes, respectively
I_{xz}	= cross product of inertia in X-Z plane
m	= aircraft mass
p,q,r	= body axis roll, pitch, and yaw rates, respectively
$\dot{p},\dot{q},\dot{r}$	= body axes roll, pitch, and yaw accelerations, respectively
Q	= dynamic pressure
S	= reference wing area
$V_T, \dot{V}_T$	= flight path total airspeed and time rate of change of airspeed
α	= angle of attack (AOA)
β	= angle of sideslip
$\delta_a, \delta_e, \delta_r$	= aileron, elevator, and rudder control surface deflections, respectively
θ, ϕ	= pitch and roll euler angles

Presented as Paper 75-33 at the AIAA 13th Aerospace Sciences Meeting, Pasadena, Calif., Jan. 20-22, 1975; submitted Feb. 18, 1975; revision received June 16, 1975.

Index categories: Aircraft Handling, Stability, and Control; Computer Technology and Computer Simulation Techniques.

*Lead Handling Qualities Engineer, A-10 System Program Office.

†Handling Qualities Engineer, ASD Airframe Engineering.

Introduction

THE A-10 is a single-placed close air support aircraft manufactured by Fairchild Republic Company, Farmingdale, N.Y. (Fig. 1). The aircraft is a low-wing, low-tail configuration with two high-bypass turbofan engines. The aircraft maximum gross weight is approximately 38,000 lb with the GAU-8, 30-mm cannon and without external stores. It has a maximum level flight airspeed in excess of 400 knots true airspeed.

A spin flight test program was initiated with the prototype A-10 aircraft in November 1974 at Edwards Air Force Base, Calif. Its planning and conduct followed the guidelines of Ref. 1. The analysis of this paper preceded and supported the flight test program. It was based upon a hybrid computer simulation of A-10 dynamics for prediction of aircraft susceptibility to entry into out-of-control or spin conditions. Since existing information from flight tests documented flight characteristics up to stall angles of attack and NASA Langley vertical spin tunnel tests[2] defined fully developed spin and recovery characteristics, this effort concentrated on vehicle dynamics associated with various control misapplications between stall and fully developed spin angles of attack. The results of this study effort helped guide the planning and conduct of the flight test program.

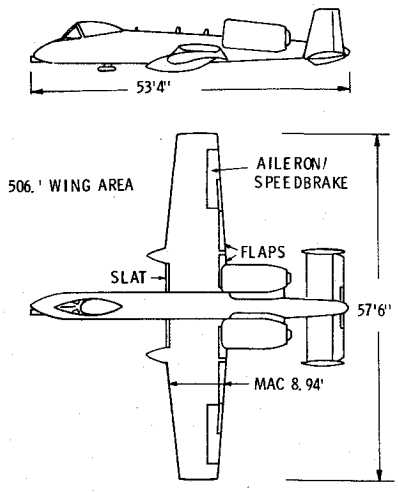

Fig. 1 A-10 aircraft.

Technical Approach

The detailed and thorough real-time hybrid computer simulation of aircraft stall/poststall/spin dynamics required considerable wind-tunnel data collection, processing, and computer software preparation. Fairchild Republic Company collected and provided all force and moment and damping derivative data for input into the mathematical model; the Stability and Control Branch (ENFDH) of Aeronautical Systems Division (ASD), along with ASD Computer Center personnel, formed the computer software programs and conducted this analysis.

The hybrid computer consisted of a Comcor Ci-5000 analog coupled with a Xerox Sigma 7 digital computer. The computer simultaneously solved, in real time, the six-degree-of-freedom body axes equations of motion. Programmed and pilot-in-the-loop control inputs were used as forcing functions for aircraft motions. For pilot-in-the-loop control, a console controller, consisting of individual engine throttle controls, seven instruments, and a stick for normal pitch and roll commands, which rotated for rudder inputs, was used to perform a variety of operational maneuvers. The computer program was structured to accept wind-tunnel data in stability derivative form as functions of angle of attack, sideslip, Mach number, and control surface position. All damping and cross-damping stability derivatives were computed analytically, based upon component wind-tunnel tests in accordance with the analytical methods of Ref. 3. Engine stall, engine gyroscopic coupling, and the A-10 stability augmentation system (SAS) were modeled by computer software. The engine stall model assumed single or dual flameout whenever transient angle of attack exceeded stall by 7°. The stability augmentation system consisted of a pitch rate damper with 2° elevator authority, no aileron SAS, and a rudder SAS with 10° authority. The rudder SAS consisted of a blend of yaw rate damping, aileron/rudder interconnect, and lateral acceleration fixed gain signals. Separate wind-tunnel aerodynamic data computer tapes were used to evaluate A-10 clean, flap, speedbrake, and external store configurations.

Wind-Tunnel Data

The majority of wind-tunnel data were obtained from the NASA Ames 12-ft pressure tunnel at a Mach number of 0.2 and a Reynolds number (per foot) of 3.51×10^6, with 1/10- and 1/20-scale models of the prototype A-10 aircraft. Data were collected in 5° and 10° angle-of-attack increments from −4° to 90° angle of attack (AOA) and with sideslip combinations from −10° to 30°. Additional data at 40° sideslip, at below stall angle of attack, were obtained from the Convair (San Diego) low-speed wind tunnel using a 1/10-scale model A-10. Wind-tunnel data were extrapolated to 50° sideslip for simulation use.

Presimulation Analysis

Presimulation analysis of wind-tunnel data was conducted to provide an insight into spin susceptibility and assist computer simulation studies. Pitch and directional stability (C_{m_α} and C_{n_β} derivatives) and control power characteristics were evaluated to determine angle of attack where stability deteriorated or control effectiveness reversed. For the clean configured A-10, pitch stability was restoring at all angle of attack to 90°, at the aft permissible center of gravity of 30% mean aerodynamic chord (m.a.c.). Body axis rudder power was positive (negative $C_{n_{\delta_r}}$) to 45° angle of attack and 20° sideslip. Roll control effectiveness $C_{l_{\delta_a}}$ was reduced significantly at stall angle of attack but remained in a positive sense to 60° AOA. Yaw due to aileron $C_{n_{\delta_a}}$ was proverse to 30° AOA, where it crossed zero and remained adverse to 90° AOA. Directional stability C_{n_β} was restoring to 60° angle of attack at sideslip angles to 10°. Elevator power $C_{m_{\delta_e}}$ remained in a positive sense to 90°. These characteristics alone suggested a strong resistance to departure and positive aircraft controllability to angles of attack considerably above stall. Stall angles of attack, defined by the first break in lift coefficient, varied from 20° at 0.2 Mach number to 14° at 0.6 Mach number.

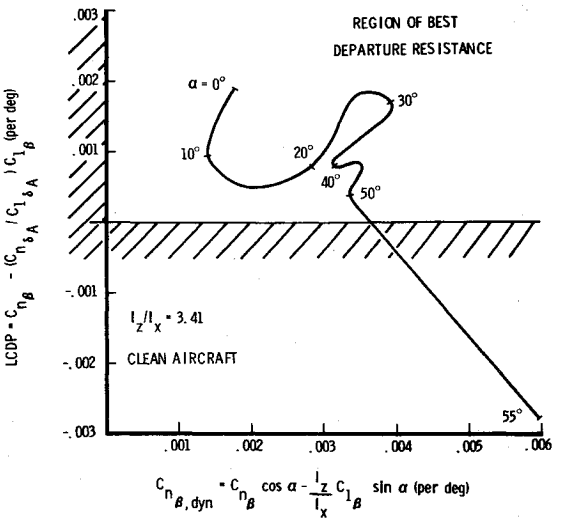

Fig. 2 Departure criteria.

The departure criterion of the Lateral Control Departure Parameter (LCDP) was plotted vs $C_{n_{\beta_{DYN}}}$ for the clean configured aircraft in Fig. 2 as defined in Refs. 3 and 4. The inertial ratio of 3.41 corresponds to an aircraft gross weight of 33,050 lb for the operational, cruise-configured A-10. LCDP is a divergence criterion when roll control is used; negative values of this parameter indicate a roll reversal tendency. This parameter was positive to over 50° for the clean aircraft. The values of both parameters suggest that the A-10 has good departure resistant properties.

Simulation Investigation

This simulation effort, like the flight test program, was patterned after Ref. 1. This specification structures flight testing into four phases; each progressive phase of testing calls for increasing time duration of misapplied control inputs at stall. Phase A requires immediate recovery at stall; phase B involves aggravated (briefly misapplied) control inputs at stall; phase C calls for stalls with aggravated and sustained control inputs for 3 sec; and phase D requires sustained and aggravated control inputs for up to 15 sec or three spin turns, whichever is longer. This analysis focused on spin susceptibility from 1-g trim flight for the clean configured A-10; however, flaps, speedbrakes, symmetric, and asymmetric external store configurations also were evaluated. The store asymmetry evaluated consisted of one MK-84 laser bomb at pylon station 144, which resulted in a roll moment asymmetry of 27,718 ft-lb. The effects of stability augmentation, power, and center of gravity also were considered.

This simulation analysis was conducted in four parts (phases). The first two phases evaluated spin susceptibility, from 1-g trim flight, with 15 sec of misapplied control inputs for the clean-configured A-10. Also identified were spin modes achievable from other than 1-g trim or accelerated flight conditions. This technique of analysis simulated the NASA Langley vertical spin tunnel test method, where the model (in this case, the computer solution) was initialized at various high yaw rate and angle-of-attack combinations and then allowed to seek a spin or no-spin condition. The third Phase of study addressed spin susceptibility relative to phase C (3 sec) misapplied control imputs. With minor exception, these three study phases were conducted with stability augmentation disconnected (SAS off), since the A-10 production SAS had not been finalized. The A-10 SAS was, however, defined prior to the fourth phase of analysis effort. This

phase addressed the impact of the SAS on spin as well as the A-10 configured with a single asymmetric store loading of one MK-84 laser bomb.

Spin entry was initiated at altitudes of 15,000 and 25,000 ft. Control imputs were generally full authority and consisted of separate elevator, aileron, rudder, and coordinated and uncoordinated rudder and aileron combinations. Full authority elevator control imputs generally were made simultaneous with all lateral-directional inputs.

General Results

Stall, poststall, spin, and recovery characteristics were evaluated for various A-10 configurations with a matrix of misapplied control imputs at 1-*g* trim and accelerated flight conditions. All Phase C (3 sec) misapplied control inputs during 1-*g* trim and accelerated flight maneuvers, for all configurations evaluated at forward and aft c.g., with SAS on or off, resulted in poststall gyrations but no spins when all controls were neutralized at 3 sec for recovery. This analysis result has been verified in the flight test program, during which greater than 200 Phase-C-type maneuvers have been performed at a variety of flight conditions with various configurations without spin occurrence. Three spin modes were obtained during phase D (15 sec) simulation studies: a low angle of attack, an intermediate angle of attack, and a high angle-of-attack spin mode. For all configurations, with the exception of full speedbrake deflection, only the low angle-of-attack spin mode was obtained during phase D or pilot-in-the-loop misapplied control inputs from 1-*g* trim or accelerated flight conditions. With full speedbrake, a low- and an intermediate angle-of-attack spin mode were obtained. The high angle-of-attack and intermediate spin modes for the remaining A-10 configurations evaluated were obtained with a simulation technique that parallelled the NASA Langley vertical spin tunnel tests. This consisted of initializing the computer solution at high yaw rate and angle-of-attack combinations (greater than those that were attained during maneuvering flight situations) and then allowing the simulation to seek a spin or no-spin condition in an operate mode. Abrupt control application of full authority elevator, rudder, aileron, or coordinated roll/yaw controls resulted in transient sideslip dynamics with 50°, a maximum value of accepted applicability of the wind-tunnel data. Abrupt control application of full authority cross (uncoordinated) roll/yaw controls resulted in transient sideslip response greater than 50° at 1 *g* and accelerated maneuver flight conditions.

Recoveries from the low angle-of-attack mode were abrupt within one turn using either 1) all neutral controls, 2) rudder against the spin with neutral aileron and elevator, or 3) rudder against the spin and aileron with the spin (crossed controls) with neutral elevator. Recoveries from the intermediate spin mode occurred within two turns at neutral aileron and elevator with opposite rudder. Recoveries from the high-angle-of-attack spin mode were greater than five turns (unacceptable) using full authority cross roll/yaw controls of rudder against the spin direction and aileron with the spin. Full forward, neutral, and full aft elevator deflection in combination with these controls did not change this five-turn recovery result appreciably. Slight changes to the baseline aerodynamicis of rudder sensitivity $C_{n_{\delta_r}}$ or yaw rate damping C_{n_r} resulted in satisfactory recoveries (less than two turns) with the previously maintained control inputs. The sensitivity of these results on spin and recovery were evaluated by systematically changing baseline aerodynamic derivatives by 25, 50, and 100% nominal values. Their effects will be discussed further.

Spin Characteristics

The low angle-of-attack spin mode exhibited angles of attack from 30°-35°, with inertial turn rates from 40 to 60 deg/sec and descent velocities of 320-380 fps. This mode could be entered with either rudder alone, full coordinated rudder and aileron, or full uncoordinated roll/yaw controls at full aft pitch control position and required approximately 15 sec to develop fully. The spin occurred in the direction of rudder pedal input with the exception of the uncoordinated roll/yaw spin, which was in the direction of roll control input. Entry controls were simultaneous and abrupt with the exception of uncoordinated (cross) roll/yaw control inputs. The uncoordinated roll and yaw entry control inputs were performed slowly (10 sec to full authority) in order to maintain transient sideslip values within the acceptable aerodynamic data limit of 50°. The characteristics of this spin mode agree well with NASA Langley vertical spin tunnel results.[2] The intermediate spin mode, with full speedbrake, occurred at angle of attack from 50°-55° with a spin rate of 50-60 deg/sec at a vertical velocity of 250 fps. It was entered with a pilot-in-the-loop technique from 1-*g* trim flight with slow application of uncoordinated roll/yaw controls at full aft pitch control position. The intermediate spin mode, for all other configurations evaluated, was more oscillatory in angle of attack and rates than that experienced with the full speedbrake. It exhibited angles of attack from 55°-70° with a yaw rate of 70-80 deg/sec (Fig. 3). It was obtained only with uncoordinated roll/yaw controls at initial conditions of high yaw rate and angle of attack and was not attainable during 1-*g* trim or maneuvering flight. The high angle-of-attack spin mode occurred at 80°-84° angle of attack, yaw rates of 150-160 deg/sec at descent velocities of 200-250 fps for the cruise-configured A-10 (Fig. 3). It was smooth with low oscillations and was obtained with cross roll/yaw controls at full aft pitch control position resulting from initialized conditions of high yaw rate and angle of attack. It also could not be obtained with misapplication of controls from 1-*g* or accelerated flight conditions. Full coordinated roll/yaw control positions were evaluated at yaw rate and angle-of-attack combinations that had resulted in the intermediate and high-angle-of-attack spin modes when using uncoordinated (cross) roll/yaw controls. In these instances, the dynamics degenerated into the low angle-of-attack spin mode shown in Fig. 3, which consistently had

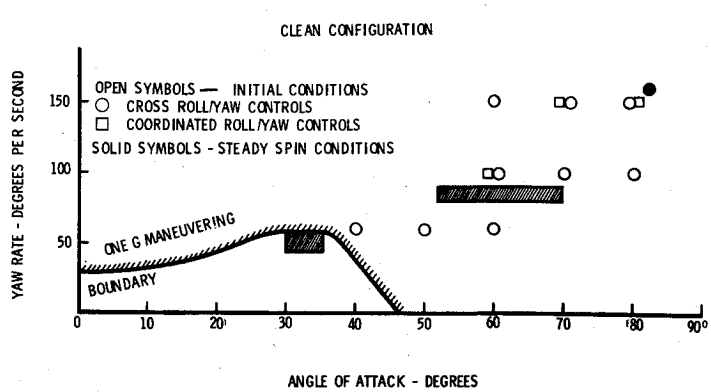

Fig. 3 Developed spin modes.

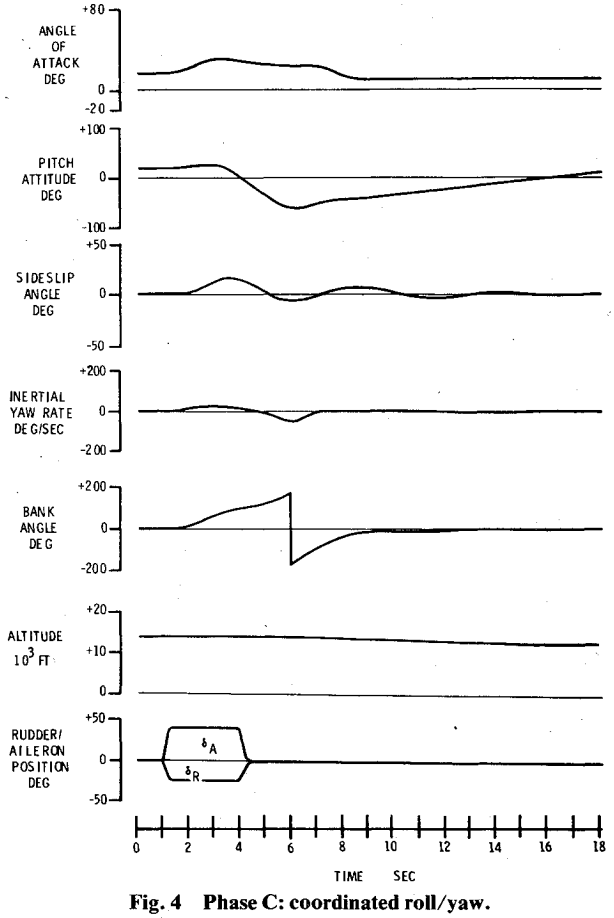

Fig. 4 Phase C: coordinated roll/yaw.

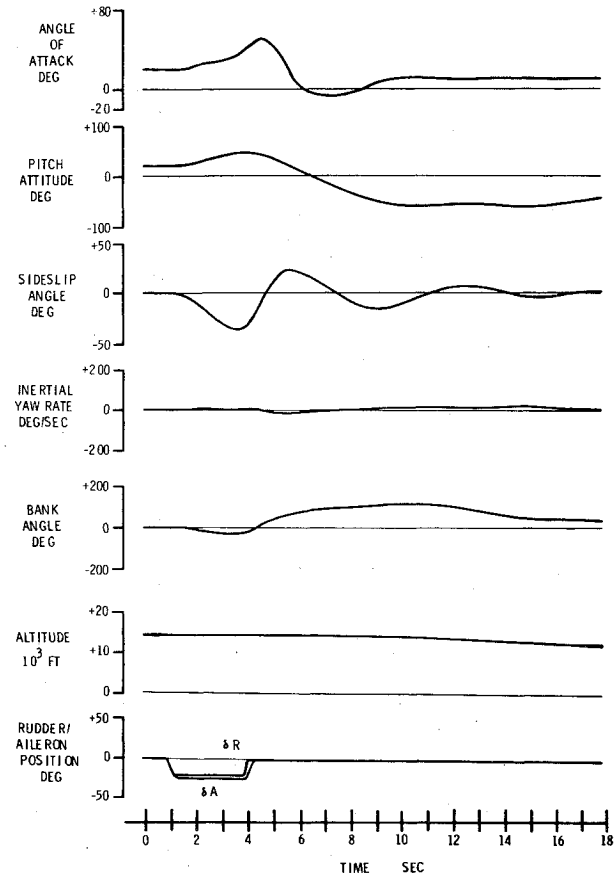

Fig. 5 Phase C: uncoordinated roll/yaw.

resulted during Phase D misapplied controls from 1-g and maneuver flight conditions.

These spin entry, spin, and recovery characteristics were essentially the same with leading-edge slats in or out, SAS on or off, and the engine stall model operative or inoperative. The one exception to this statement concerned phase D aileron-only inputs; with SAS on, the low angle-of-attack spin developed, whereas, with SAS off, it was not obtained. This occurrence was attributed to the dominant nature of the aileron-to-rudder interconnect. This fixed-gain, zero-lag, SAS loop inputs rudder proportional to aileron primarily to coordinate abrupt rolling maneuvers. Gyroscopic engine coupling was evaluated during abrupt symmetric pullups from 1-g trim flight. Roll and yaw rate peak transient values were less than 5 deg/sec with minimal sideslip excursions; consequently, their impact on spin entry was considered negligible.

Discussion of Time Histories

Figures 4 and 5 present typical results of phase C (3 sec) misapplied control inputs. Figure 4 shows the dynamics associated with abrupt application of right coordinated full authority rudder and aileron from 1-g trim conditions of 15,000 ft at an airspeed of 225 fps. Figure 5 presents the aircraft motion associated with uncoordinated roll/yaw controls of full right rudder pedal and partial left roll control at this same flight condition. The poststall dynamics resulting from these control misapplications are described best with reference to inertial coupling, kinematic coupling, control power, and stability. To clarify these terms, the three body axes rotational equations of motion and two of the three translational equations of motion for the center of mass of the aircraft are presented[5]

$$\dot{p}=\frac{(I_y-I_z)}{I_x}\,qr+\frac{I_{xz}}{I_x}(\dot{r}+pq)+\frac{QSb}{I_x}(C_l) \qquad (1)$$

$$\dot{q}=\frac{(I_z-I_x)}{I_y}\,pr+\frac{I_{xz}}{I_y}(r^2-p^2)+\frac{QS\bar{c}}{I_y}(C_m) \qquad (2)$$

$$\dot{r}=\frac{(I_x-I_y)}{I_z}\,pq+\frac{I_{xz}}{I_z}(\dot{p}-qr)+\frac{QSb}{I_z}(C_n) \qquad (3)$$

$$\dot{\alpha}=\frac{1}{\cos\beta\cos\alpha}\left(-p\sin\beta+\dot{\beta}\sin\beta\sin\alpha+\frac{g}{V_T}\cos\theta\cos\phi-\frac{QS}{mV_T}(C_N)\right)+q-\frac{\dot{V}_T}{V_T}\tan\alpha \qquad (4)$$

$$\dot{\beta}=p\sin\alpha-r\cos\alpha+\frac{g}{V_T}\,\frac{\cos\theta\sin\phi}{\cos\beta}-\frac{\dot{V}_T}{V_T}\tan\beta+\frac{QS}{mV_T\cos\beta}(C_y) \qquad (5)$$

The first two terms of the $\dot{p}$, $\dot{q}$, and $\dot{r}$ equations are considered the inertial coupling terms of the rotational equations of motion; the remaining terms in these equations represent the aerodynamic effects. The first two terms in the $\dot{\alpha}$ and $\dot{\beta}$ equations are considered the kinematic coupling terms. The remaining terms of Eqs. (4) and (5) account for gravitational, aerodynamic, rate, and flight path acceleration effects.

The inertial coupling terms of Eqs. (1-3) (neglecting I_{xz} effects) cause accelerations in either pitch, roll, or yaw ($\dot{q}$, $\dot{p}$, $\dot{r}$, respectively) as a consequence of rates generated about the other two orthogonal axes. The magnitude of these accelerations are a function of inertial properties I_x, I_y, and I_z. Representative values for these inertias for the clean-configured A-10 at a gross weight of 33,050 lb and 30% m.a.c. are 132,500, 52,510, and 179,000 slug-ft^2 in pitch, roll, and yaw, respectively. These inertial coupling terms were used

to analyze simulation dynamics to determine the significance of coupling on transient motion. These accelerations generally opposed desired pilot aircraft motion during abrupt maneuvers.

The kinematic coupling of Eqs. (4) and (5) is thought of most easily as the geometric interchange of angle of attack and sideslip during rolls at high angle of attack. An inspection of these terms will show that pilot use of an effective aileron alone at high AOA will cause adverse sideslip (aircraft nose away from the roll) in accord with the term $p \sin\alpha$ [Eq. (5)]. This high sideslip along with high roll rate also will cause kinematic coupling in angle of attack in accord with $-p \sin\beta$ [Eq. (4)]. In this case, positive aileron effectiveness caused adverse sideslip, which resulted in an aircraft-nose-down angle of attack change due to kinematic coupling. This characteristic was precisely what happened during these studies using abrupt aileron-alone inputs at high angle of attack. The aerodynamic terms of Eqs. (4) and (5) also were significant during these studies. Pitch, roll, and yaw control power characteristics dominated the transient response by comparison to the aerodynamic rate damping and stability terms.

Figures 4 and 5 illustrate the results mentioned previously which stated that 3 sec of misapplied control inputs, followed by all neutral controls, do not result in a spin conditon. The initial yaw rate and roll angles of Fig. 4 for full authority right coordinated roll/yaw control inputs show positive response in the direction of control inputs. The initial peak in sideslip was in the adverse sense and indicates a maneuver that was not totally coordinated. In this case, the kinematic coupling in sideslip was due to the roll rate term ($p \sin\alpha$) exceeding the yaw rate term ($-r \cos\alpha$). The rudder used did not generate sufficient yaw rate to reduce the adverse sideslip generated by roll rate and therby coordinate the maneuver at low sideslip values. Adverse yaw due to aileron $C_{n_{\delta_a}}$ contributed to the magnitude of adverse yaw indicated but was of secondary effect by comparison with control power and kinematic coupling aspects. The initial peak sideslip response of Fig. 5, for the uncoordinated Phase C roll and yaw inputs of right rudder pedal and left roll stick, was opposite that of the coordinated control input results of Fig. 5. This again is explained primarily by means of kinematic coupling in sideslip due to the lack of harmony in initial roll and yaw rates generated by rudder and aileron control inputs. The initially higher peak sideslip of Fig. 5 occurred because sideslip obtained with rudder was additive to that generated by roll rate. The aircraft nose-right rudder pedal generated a negative (nose-right) sideslip, and the left roll stick input ($-\delta_a$) also generated a negative sideslip, as expressed by the kinematic coupling terms of Eq. (5). The greater transient peak value in angle of attack of Fig. 5, as compared to Fig. 4, was due in part to kinematic coupling. The rate increase in angle of attack of Fig. 5 at 3 sec corresponds in sign and magnitude with the Eq. (4) term, $-p \sin\beta$. Further signs of kinematic coupling effects in angle of attack are evidenced by local zero slopes in angle of attack at instances where either roll rate or sideslip becomes zero.

Figure 6 shows the low angle-of-attack spin mode experienced when full and abrupt coordinated roll and yaw controls were maintained for 15 sec or longer. Elevator input is not shown but was input simultaneously to full trailing edge up with roll/yaw control application and returned to neutral with roll/yaw neutral controls. At approximately 20 sec, the spin is fully developed. Beyond this time period, yaw rate remains constant at 50 deg/sec, and the aircraft flight path is vertical as indicated by angle of attack and pitch angle, which sum to 90°. The first 5 sec of response in Fig. 6 is very similar to the Phase C coordinated aileron and rudder response of Fig. 5. After 5 sec, however, another buildup in angle of attack occurs; this is due primarily to inertial coupling in pitch. At this point, positive roll and yaw rates (body axes) caused a positive pitch acceleration, resulting in a positive pitch rate and positive change in angle of attack in accord with the Eq. (2) term. The immediate recovery, with all neutral controls,

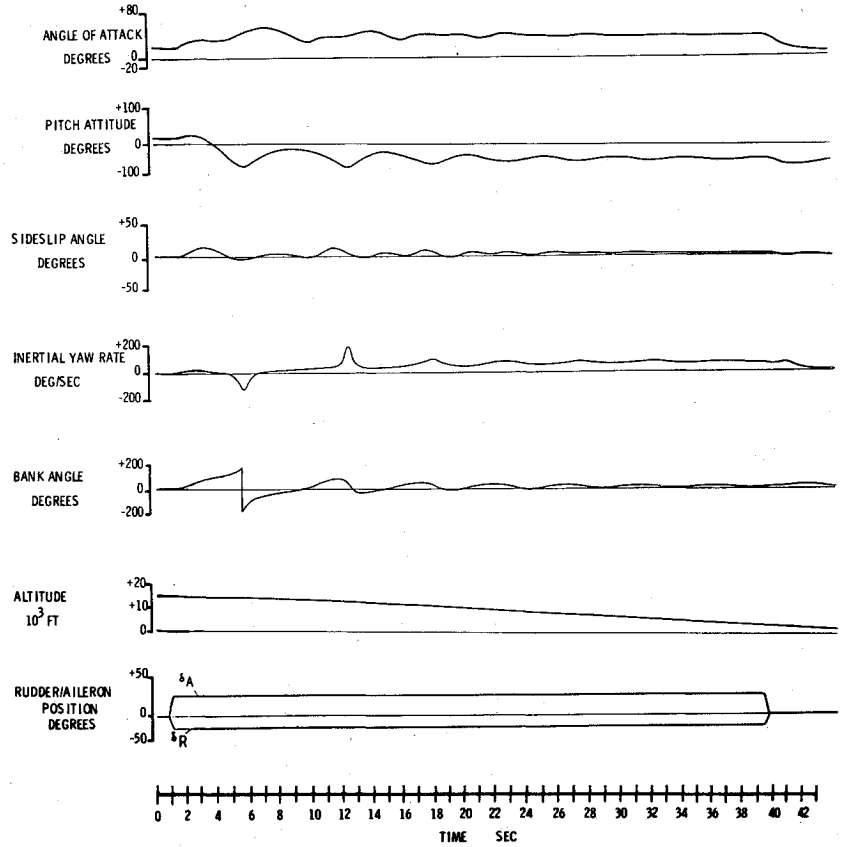

Fig. 6 Phase D: coordinated roll/yaw.

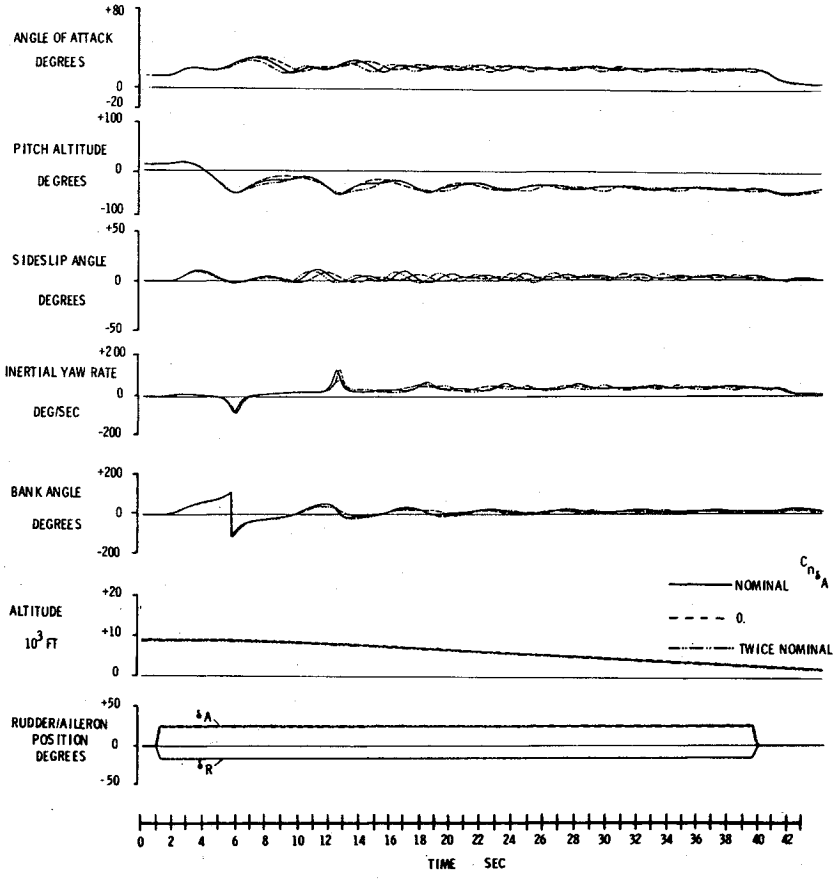

Fig. 7 Effect of yaw due to aileron.

beyond 41 sec also is shown. This same low angle-of-attack spin mode also was obtained with slow application of cross (uncoordinated) roll/yaw controls. For this case, however, the direction of spin was opposite the direction of rudder pedal input: in the direction of roll control input.

Aerodynamic Parametrics

Changes to baseline A-10 aerodynamics of as much as 50% and 100% were made, and their effects on spin entry, spin, and recovery were evaluated. Changes were made to yaw-due-to-aileron $C_{n\delta_a}$, roll and yaw control effectiveness $C_{l\delta_a}$ and $C_{n\delta_r}$, yaw and pitch rate damping C_{n_r} and C_{m_q}, and cross-damping derivatives C_{l_r} and C_{n_p}. Aircraft flight test results had shown values of roll performance less than that predicted using wind-tunnel values of aileron effectiveness. Consequently, the majority of this analysis was performed with 80% baseline wind-tunnel values of roll sensitivity $C_{l\delta_a}$. Figure 7 is an example of the results of these parametric studies. In this instance, adverse yaw-due-to-aileron $C_{n\delta_a}$ was increased and reduced 100% from nominal wind-tunnel values. This figure shows the insignificant effect that this relatively large percentage change had on spin entry, spin, or recovery from the low angle-of-attack spin mode using right-coordinated roll/yaw controls. Adverse yaw impact on the high angle-of-attack spin mode and its recovery also were examined. Baseline $C_{n\delta_a}$ (-0.0004/deg at 65° AOA) was increased and decreased 50% for all angles of attack above 65°. It had an insignificant impact on the high-AOA spin mode or its recovery.

The remaining aerodynamic derivative changes discussed caused minor differences in vehicle dynamic motion with regard to spin existence or recovery with a particular set of control inputs, with one exception: recovery from the high angle-of-attack spin mode. As previously mentioned, recovery from this mode with nominal wind-tunnel aerodynamics was greater than five turns using full antispin roll/yaw controls of rudder against the spin direction and aileron into the spin. Recoveries from this mode were satisfactory (<3 turns) when relatively small changes were made to nominal values of either rudder sensitivity $C_{n_{\delta_r}}$ or yaw rate damping C_{n_r}. Recoveries were satisfactory when $C_{n_{\delta_r}}$ was biased by a value of -0.00025/deg above 65°AOA from a nominal value of $+0.00015$/deg at 65° AOA. Recoveries also were satisfactory when C_{n_r} was biased (negatively) by a fixed increment of -0.05/rad above 65° AOA from a nominal value of -0.1/rad at 65° AOA.

Flight Test Correlation

Over 45 program flights have been accomplished with the prototype A-10 aircraft at this time. Approximately 200 Phase C (3 sec misapplied controls) maneuvers and 50 spins and recoveries have been performed with various configurations at 1-g and accelerated flight conditions. It is not the intent of this article to present a detailed comparison of simulation and flight test results; however, obvious areas of agreement and disagreement can be noted. Phase C flight test results thoroughly substantiated simulation predictions that indicated no susceptibility to spin with 3 sec of misapplied control inputs at stall when using all neutral controls for recovery. Rudder-alone and coordinated roll/yaw controls at full aft pitch control position during flight testing resulted in developed spin conditions when controls were maintained beyond 8-10 sec. This mode was recoverable easily using all neutral controls, rudder-alone at neutral aileron and elevator, and cross roll/yaw controls. This flight test mode, for the cruise-configured A-10, was more oscillatory in angle of attack, 45°-55°, with higher inertial yaw rate, 65-70 deg/sec, than the low angle-of-attack spin mode predicted by this analysis. Abrupt and sustained application of uncoordinated roll/yaw controls from 1-g trim and accelerated flight con-

ditions in the test program resulted in violent poststall gyrations, with transient sideslips in excess of 50°, and they were terminated at 15 sec without the development of any obvious spin mode. Simulation results indicated the same trend. A high angle-of-attack spin mode was experienced in flight with 40% speedbrake during intended "high spin mode investigations." It was obtained by cross-control application of aileron at one turn into a spin entered from 1 *g* using full rudder at full aft pitch control position with neutral aileron. This high angle-of-attack flight test mode occurred at 75°-80° AOA with a turn rate of 80-90 deg/sec and was recovered at 2¼ turns with full opposite rudder at neutral elevator and aileron. The full speedbrake spin mode experienced during flight tests was similar to the low angle-of-attack spin mode identified in this text. It was entered with rudder alone at full aft pitch control and exhibited angle of attack of 35°-45° at inertial yaw rates of 40-45 deg/sec. Its recovery was within one turn using all-neutral controls.

Conclusions

This analysis predicted the existence of three spin modes for the A-10 aircraft for various configurations, i.e., cruise, 30° flaps, full speedbrake, and symmetric and asymmetric external store loadings. Only the low-angle-of-attack spin mode resulted from Phase D (15 sec) misapplied control inputs from 1-*g* or accelerated flight conditions, with the exception of the full speedbrake configuration, for which an intermediate spin mode was encountered with misapplied control inputs at 1-*g* trim flight. The intermediate and high angle-of-attack spin modes, for the remaining configurations investigated during this analysis, were obtained only by initializing the computer solution artificially at high yaw rate/AOA combinations. Recoveries from all but the high angle-of-attack and intermediate-spin modes obtained were not affected noticeably by similar changes to either yaw rate damping or rudder power. This large aerodynamic sensitivity to recovery from the high angle-of-attack spin mode reduced the confidence of these analytical results regarding recovery from this spin mode.

Spin entry, spin, and recovery were influenced primarily by control power characteristics as compared to the effects of static stability or dynamic derivative terms. The exception to this regarded recovery from the high angle-of-attack spin mode, which was very sensitive to changes in yaw rate damping. Control combinations, length of application, and authorities dictated the magnitude and occurrence of poststall gyrations and spin conditions.

The lack of adequate wind-tunnel data at high sideslip (40°-70°) restricted this analysis effort regarding definition of vehicle dynamics associated with abrupt cross (uncoordinated) roll/yaw control inputs. Wind-tunnel data to 40° sideslip probably would have been adequate for these studies were it not for the highly effective control powers of the rudder and aileron of the A-10 aircraft.

These simulation results proved to be reasonably accurate by comparison with flight test results for Phase C and D testing. Their application during flight test planning and conduct (in which this author was a participant) significantly improved overall program efficiency. Flight testing during Phases A and B was minimized due in part to these results, which indicated no possibility of spin occurrence. Phase C and D flight tests of center of gravity, SAS, and the matrix of misapplied control inputs also were minimized as a consequence of these studies.

References

[1] "Stall/Post-Stall/Spin Flight Test Demonstration Requirements for Airplanes," 1972, MIL-S-83691A, U.S. Air Force Military Specification.

[2] Scher, S.H. and White, W.L., "Spin Tunnel Investigation of a 1/30-Scale Model of the Fairchild A-10A Airplane," NASA TM SX-3090, 1974.

[3] Weissman, R., "Criteria for Predicting Spin Susceptibility of Fighter-Type Aircraft," Aeronautical Systems Division, Wright Patterson AFB, Ohio, ASD TR-72-48, 1972.

[4] Moul, M.T. and Paulson, J.W., "Dynamic Lateral Behavior of High-Performance Aircraft," NACA RM LS8E16, 1958.

[5] Casteil, G.R., Collins, R.A., and Wykes, J.H., "An Analytical Study of the Dynamics of Spinning Aircraft," Wright Air Development Center, Wright Patterson AFB, Ohio, TR 58-381, 1958.